Schlieren visualization of water natural convection in a vertical ribbed channel

2015 J. Phys.: Conf. Ser. 655 012005

(http://iopscience.iop.org/1742-6596/655/1/012005)

Journal of Physics: Conference Series **655** (2015) 012005 doi:10.1088/1742-6596/655/1/012005

Schlieren visualization of water natural convection in a vertical ribbed channel

M Fossa, M Misale, G Tanda[1]
DIME, Università degli Studi di Genova, Genova, Italy

Abstract. Schlieren techniques are valuable tools for the qualitative and quantitative visualizations of flows in a wide range of scientific and engineering disciplines. A large number of schlieren systems have been developed and documented in the literature; majority of applications involve flows of gases, typically air. In this work, a schlieren technique is applied to visualize the buoyancy-induced flow inside vertical ribbed channels using water as convective fluid. The test section consists of a vertical plate made of two thin sheets of chrome-plated copper with a foil heater sandwiched between them; the external sides of the plate are roughened with transverse, square-cross-sectioned ribs. Two parallel vertical walls, smooth and unheated, form with the heated ribbed plate two adjacent, identical and asymmetrically heated, vertical channels. Results include flow schlieren visualizations with colour-band filters, reconstructions of the local heat transfer coefficient distributions along the ribbed surfaces and comparisons with past experiments performed using air as working fluid.

1. Introduction

The schlieren technique introduced by Foucault [1] and Toepler [2] has long been an attractive diagnostic tool for the study of fluid flow fields. Since the schlieren effect is related to gradients of the refractive index, density/temperature variations in a fluid flow can be easily visualized by means of this optical method, basically requiring a white light source, an optical setup made of mirrors or lenses, a camera and a special filter to detect the light deflections in the observed field. A comprehensive and exhaustive description of the schlieren technique, including qualitative and quantitative applications, optical principles and devices to detect light deflections, is provided in the book by Settles [3].

Due to the simple relationship between the refractive index and the density of gases, the schlieren technique has been mainly employed for the investigation of flow and thermal fields using a gas as flowing medium [3]. Conversely, schlieren was not a popular method in the past to visualize liquid flows. Liquids usually induce strong light refractions and this limits the use of schlieren devices, which do not typically need or want high sensitivity, to phenomena characterized by very small changes in temperature or a very small width of the test section in the light beam direction. In addition, quantitative results can be gained if the refractive index variations with the liquid temperature and pressure are precisely known *a priori*.

The Authors of the present work were apparently the first to apply a quantitative schlieren technique to the study of heat transfer in liquid flows [4-5]; in particular, local heat transfer

[1] To whom any correspondence should be addressed. E-mail: giovanni.tanda@unige.it

coefficients along a vertical plate in the presence of laminar, natural convective water flow have been determined. Results have been compared with numerical simulations, theoretical relationships and literature experimental data obtained in air by the same technique and under similar conditions in terms of dimensionless groups. The experiments performed proved the validity of the experimental method and its applicability to the study of thermal fields not only in gases but even in transparent liquid flows. This work aims at gaining qualitative and quantitative visualization of natural convection in water channels having repeated ribs on the heat transfer surfaces. These surfaces are commonly encountered in several engineering applications (electronic equipment, solar collectors, passive heating of buildings, etc.). The roughening of a heat transfer surface is a common practice to increase the convective heat transfer [6-10]. Roughness elements may significantly affect the free convection heat transfer in vertical channels owing to the following circumstances: (i) the blockage effect associated with the presence of protrusions could provoke a weaker induced flow, potentially reducing the heat transfer; (ii) the roughness could induce disturbances in the overlying laminar boundary layer, thus causing premature transition to turbulence; (iii) the roughness elements, if heated, add an extra heat transfer surface area. Moreover, there are situations (surfaces of buildings, electronic circuit boards) in which the roughness occurs naturally and is not added for the specific purpose of modifying heat transfer performance. Thus, understanding the thermal behaviour of these systems is essential for their correct design.

2. Theoretical background

The angular deflection of a light ray due to a density/temperature gradient in a fluid layer can be estimated from geometrical optics.

Let us consider a light ray, propagating along the *z*-axis of a Cartesian *x*-*y*-*z* coordinate system, which passes through a fluid layer, of depth *L*, bounded by two surfaces lying onto *x*-*y* parallel planes, as shown in Fig.1. The deflection angle of the light ray in the *y* direction as it reaches the *x*=*L* plane is given by

$$\alpha_y = \int_0^L \frac{1}{n}\frac{\partial n}{\partial y} dz \tag{1}$$

where n is the refractive index of the fluid and the integration is performed over the entire length of the light ray in the fluid layer. Eq. (1) is derived under the assumption of very small angles of deflection.

If the phenomenon under study is two-dimensional, i.e. density/temperature of the fluid does not depend on *z*-coordinate, as the entering angle is zero, the angle at *z*=*L* is

$$\alpha_y = \frac{L}{n_0}\frac{\partial n}{\partial y} \tag{2}$$

where the term $1/n$ within the integral has been assumed not to change greatly through the test section and set equal to $1/n_0$, n_0 being a reference value for the fluid refractive index. As the gradient of the refractive index with respect to the temperature is introduced, Eq.(2) becomes

$$\alpha_y = \frac{L}{n_0}\frac{\mathrm{d}n}{\mathrm{d}T}\frac{\partial T}{\partial y} \tag{3}$$

For gases, $\mathrm{d}n/\mathrm{d}T$ can be easily deduced by applying the Gladstone-Dale and the ideal gas laws to give $\mathrm{d}n/\mathrm{d}T = -K P/(R T^2)$, where K is the Gladstone-Dale constant, R is the ideal gas constant, P is the pressure and T is the absolute temperature. For liquids, $\mathrm{d}n/\mathrm{d}T$ has to be experimentally determined. In

the case of water, Harvey et al. [11] reported the refractive index at different wavelength in the visible spectrum, versus pressure and temperature. A fitting of data, at the atmospheric pressure and averaged over the visible wavelength range, gave n_0 = 1.335 (at 20°C) and the following relationship of dn/dT with T in the 15-40°C range

$$\mathrm{d}n/\mathrm{d}T = -1.1869 \times 10^{-5} - 4.4407 \times 10^{-6}\, T + 2.5 \times 10^{-8} T^2 \quad (4)$$

where the fluid temperature T is expressed in °C. It is worthy of note that averaging dn/dT with the wavelength results in a 2% maximum deviation from Eq.(4) if any single wavelength in the visible spectrum is considered.

In the case of a water layer, enclosed by glass walls (plane and at uniform thickness) and surrounded by ambient air (at refractive index n_{air}), an additional angular deflection occurs according to Snell's law. If α'_y is the angle of the light ray as it emerges into the surrounding air after it has passed through the water layer, it follows that

$$\alpha'_y = \alpha_y \frac{n_0}{n_{air}} \quad (5)$$

where, due to the small values of the angles, sin α'_y and sin α_y have been replaced by α'_y and α_y, respectively, while (n_0/n_{air}) is the ratio between refractive indices of water and air at a standard condition (20°C, atmospheric pressure).

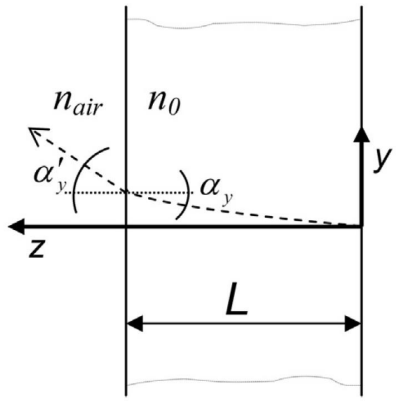

Figure 1 Deflection of a light ray due to optical disturbances in a fluid layer of depth L. Snell's law applies at the fluid/air interface if the fluid refractive index n_0 significantly differs from the air refractive index n_{air}

3. The experiment

3.1 The optical setup

The Z-type schlieren arrangement used in the present experiment is shown in Fig.2; it has been employed for quantitative heat transfer experiments in buoyancy-induced air flows for almost two decades (see, for instance, refs.[12-14]) and applied here to the study of water flows.

A noncoherent light beam coming from a 30μm-wide vertical slit source is collimated by the concave mirror M_1 to form parallel light rays crossing the test section, located inside a water chamber, whose details will be provided in Section 3.2. Without inhomogeneities of the water refractive index in the test section, the parallel light rays, focused by the concave mirror M_2, converge to a thin vertical line on the primary focal plane, representing the primary image of the light source and called primary focal line. All rays are then projected onto the screen (image plane) where a real image of the test section is formed. When inhomogeneities are present in the test section, the light rays undergo angular deflections. All rays (deflected and non-deflected) are recombined on the screen, where a non-distorted image of the test section is still formed.

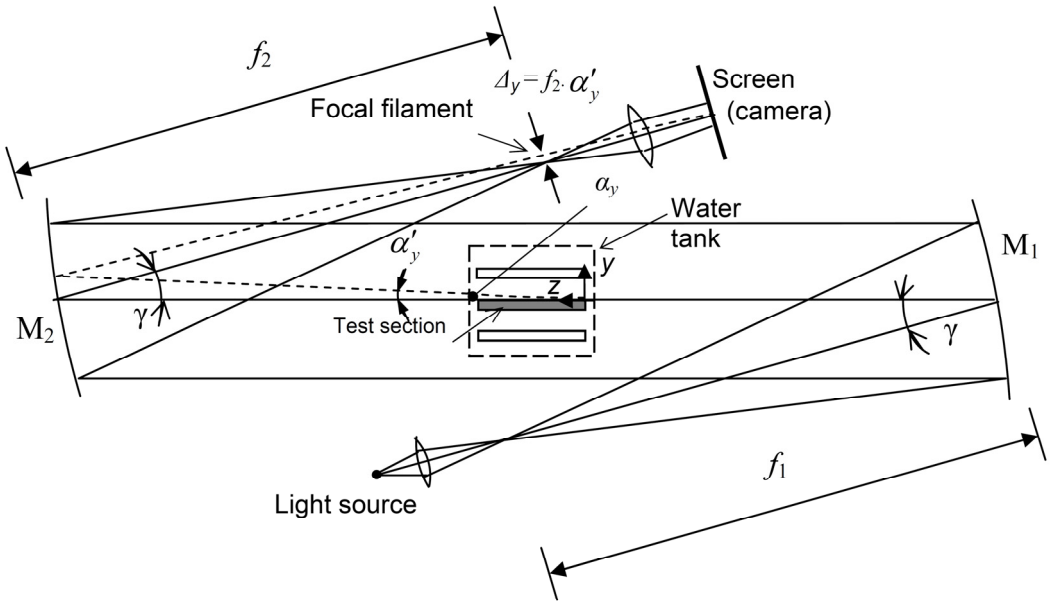

Figure 2 Schematic layout of the Z-shaped schlieren system (top view); M_1 and M_2 are 380 mm diameter concave mirrors (with focal lengths f_1 and f_2, respectively), α_y is the y-component of the light ray angular deflection within the test section, α'_y is the angular deflection of the light ray emerging into the ambient air, and Δ_y is the related shifting at the focal plane of mirror M_2 ($f_1 = f_2 =$ 1.9 m, $\gamma = 9$ deg, distance between mirrors about 8 m)

Regions of the test section that give rise to the same light angular deflection along the y direction can be identified by using a vertical filament (for instance a thin opaque strip or wire) in the primary focal plane of mirror M_2 (also called the *schlieren head*). On this plane, the deflected rays are shifted by a quantity Δ_y given by

$$\Delta_y = f_2 \alpha'_y = f_2 \alpha_y \frac{n_0}{n_{air}} \tag{6}$$

where f_2 is the distance between mirror M_2 and the primary focal line, n_{air} (=1.0003) is the refractive index of ambient (laboratory room) air and n_0 (=1.335) is the refractive index of water at a standard condition. It is useful to remind that α_y is the angular deflection, along the y direction, induced by thermal gradients in the water according to Eq.(3). In order to detect the light shifting Δ_y (and the related angular deflection), the focal filament is first placed in its reference position (position 1 in Fig.3). This position, for which the primary focal line is completely intercepted by the filament, can be clearly identified since it corresponds, without inhomogeneities in the fluid, to a uniformly dark image on the screen. Then, moving the vertical filament in the focal plane, parallel to itself, allows one to measure the values of the light ray deflections in the whole optical field. For instance, when the focal filament is shifted from position 1 to position 2 (Fig.3) by a known quantity Δ_y, a shadow is formed on the image plane. This shadow defines the locus of the images of points deflecting the light by the same angle (termed curve of equal light deflection angle or, more simply, *iso-deflection* line). When deflections of light rays passing in the vicinity of the heated wall are of interest (in order to deduce the heat transfer coefficient), the focal filament has to be shifted until its shadow, projected onto the image plane, intercepts the vertical surface profile at the desired location.

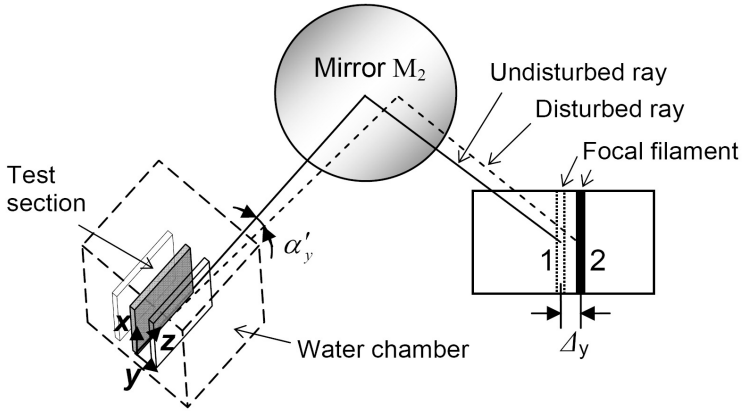

Figure 3 Measurement of the shifting Δ_y of the deflected ray in the focal plane of schlieren mirror M_2 by means of the focal filament, moved from position 1 to position 2

This schlieren technique, called *focal filament method* by Vasil'ev [15], in special conditions allows a direct measurement of the local heat transfer coefficient. For this purpose, the local convective heat transfer coefficient is now introduced

$$h = -\frac{k_w}{(T_w - T_f)}\left(\frac{\partial T}{\partial y}\right)_w \tag{7}$$

where $(\partial T/\partial y)_w$ is the fluid temperature gradient, in the direction y normal to the heated plate, evaluated at the wall, T_w is the wall temperature, k_w is the thermal conductivity of the fluid at the wall temperature and T_f is the fluid temperature.

From the combination of Eqs.(3), (5), (6) and (7), it follows that

$$h = -\frac{k_w}{(T_w - T_f)}\left(\frac{n_{air}\Delta_w}{f_2 L(\mathrm{d}n/\mathrm{d}T)_w}\right) \tag{8}$$

where the subscript w denotes quantities to be evaluated at the wall. Therefore, assuming the water properties k and $\mathrm{d}n/\mathrm{d}T$ as known, provided that T_w and T_f are independently measured, Eq.(8) states the direct relationship between the optical quantity Δ_w and the local heat transfer coefficient for a 2-D thermal field. In particular, Δ_w represents the shifting of the light ray passing in the vicinity of the heated wall and is detected by the schlieren apparatus according to the procedure illustrated in Fig.3.

A filter, operating according to the principles of the focal filament previously described, has been obtained by photographing a violet strip using a slide film. The slide produced in this manner, consisting of a 370μm-wide, transparent, violet band, was directly used as focal filament filter. As the filter is vertically mounted in the focal plane of mirror M_2, light rays deflected by the same angle pass through the violet band, and the corresponding points of the test section appear, in the image plane, coloured in violet. The width of the violet band was properly selected in order to minimize light diffraction effects and to provide a relatively high sensitivity of the technique. The use of a transparent colour band instead of an opaque band makes it easier to identify the correct location of the intersection between the iso-deflection line (appearing violet in the image plane) and the surface wall profile (appearing black in the image plane). To facilitate the description of successive steps, the violet band will be simply termed *focal filament*.

As an alternative to the focal filament method, an insight of the fluid flow/thermal field can be obtained at a glance by using a colour filter (made of a set of thin transparent coloured bands) mounted in the focal plane of mirror M_2. The colour schlieren method does not require any displacement of the filter. This method has the advantage of giving a whole-field image of the phenomenon without having to take a number of images recorded at different time steps, as occurs with the focal filament method.

Therefore, light angular deflection associated with any points framed inside the optical field can be extracted in principle from a single colour image. However, if the filter is made of discrete coloured bands, the measurement sensitivity is limited because of the finite number of bands that can be mounted on the same filter and the resulting colour images cannot typically be used for quantitative purposes.

In the present work, a colour filter with discrete bands was used only for the purpose of qualitative visualization, while the focal filament filter was used for the direct measurement of local heat transfer coefficient from Eq.(8). As previously mentioned, the present schlieren setup was originally designed for the study of convective air flows. When water is considered as convective fluid, the refraction index derivative with temperature is two orders of magnitude larger than that for air; this results in an extra-sensitivity of the optical apparatus as the fluid is changed. This problem was alleviated by properly setting the length L of the test section (in the light beam direction) and the wall-to-fluid temperature difference T_w-T_f, in order to achieve the best compromise among the sensitivity of the optical device (which increases with L and T_w-T_f), the uncertainty in the heat transfer coefficient measurement (increasing as T_w-T_f decreases), and the respect of a nearly 2-D thermal phenomenon (controlled by the extent of L).

3.2 The test section

The description of the test section used in the experiments is facilitated by the schematic view presented in Fig.4. The thermally active component of the apparatus was a vertical plate (termed *heated plate*) made of two thin sheets of chrome-plated copper with a 0.5mm-thick electric foil heater sandwiched between them. The two copper sheets were sealed with a water-resistant cement to prevent any contact between the heater and the water. When electrical power was delivered to the heater, the heated plate was expected to attain a uniform surface temperature at the steady state owing to the high thermal conductivity of copper. The dimensions of the heated plate were the following: height H = 87 mm, length L = 48 mm, overall thickness t = 8 mm. Each side of the heated plate exposed to the water flow was roughened with five transverse, square-cross-sectioned ribs, made integral with the baseplate to guarantee the absence of contact resistance. The square ribs had a height e of 2.42 mm and were regularly spaced at intervals of P = 17.4 mm, resulting in a pitch-to-height ratio P/e =7.2.

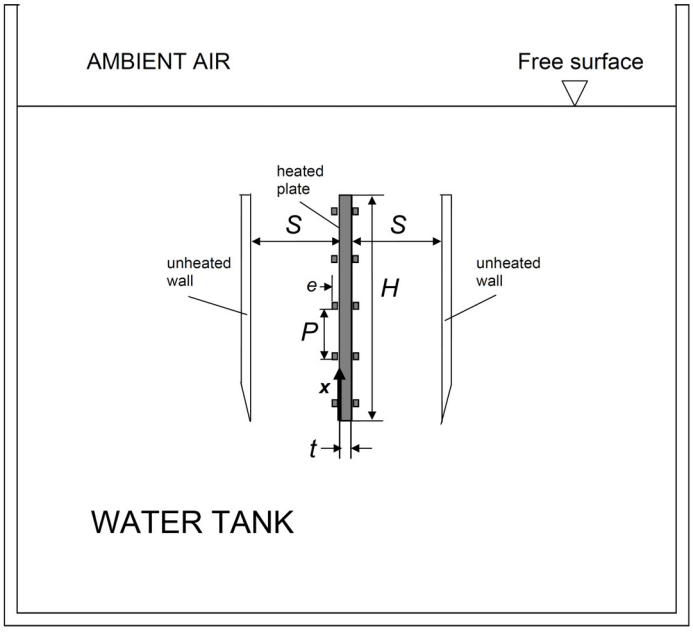

Figure 4 Schematic layout of the vertical ribbed channels inside the water tank. Drawing not to scale

Two parallel vertical walls, smooth and unheated, formed with the heated plate two adjacent, identical, and asymmetrically heated, channels. The spacing S between each unheated wall and the heated plate, set equal on both sides, was 17.4 mm, corresponding to a channel aspect ratio S/H equal to 0.2. The symmetrical arrangement of the heated plate/shrouding wall assembly permitted the optical measurements to be repeated on both sides and, owing to the symmetry, averaged at the same elevation, thus reducing the experimental error.

The heated and unheated walls were suspended, by using a supporting frame, inside a tank with inner dimensions 180x65x390 mm (width x length x height) filled with distilled water. Special care was taken in the design of the supporting frame to permit the correct positioning of the channel walls and to avoid flow obstructions in the vicinity of the channel openings. The tank was open on the top side to provide ambient pressure conditions at the air/water interface. The exit of the channel was situated 75 mm below the water surface and the entrance at 190 mm above the tank inner floor. The vertical sides of the tank normal to the light beam were made of 6mm-thick, high quality glasses so as to permit the schlieren measurements. The remaining sides and the bottom of the tank were made of 10mm-thick chrome-plated copper and finned on the ambient air side to facilitate the dissipation of the input power to the laboratory ambient air and to reduce, as much as possible, the thermal stratification in the fluid.

The heated plate and the water tank were instrumented with 0.5-mm-dia sheathed thermocouples, calibrated to ± 0.05 K. Six thermocouples were placed into the heated plate at different locations through small diameter holes drilled into the material as close to the exposed surfaces as possible. The wall temperature T_w was obtained by averaging the readings of the six thermocouples embedded in the plate material. The fluid temperature T_f was measured by a thermocouple located at the inlet section of one of the two identical channels; an additional thermocouple, able to travel vertically within the tank and outside the channels, was used to check the presence of undesirable water fluid temperature stratification.

3.3 Experimental procedure

Experiments were performed according to the following procedure:
(i) the heated plate was placed in the tank and the two unheated walls were set to provide a channel aspect ratio of 0.2;
(ii) the plate was heated by a given input of electrical power delivered to the heater, in order to achieve the desired uniform temperature over the heated plate;
(iii) at the steady state, measurements of wall and fluid temperatures were obtained by the readings of the thermocouples deployed in the material and of the thermocouple at the channel inlet, respectively;
(iv) for each run, several schlieren images were taken by moving the violet band (i.e., the focal filament) from its reference position as shown in Fig.3; the displacement impressed to the filament, directly measured by a micrometer, allows one to obtain the local heat transfer coefficients at several locations along the vertical surfaces of the heated plate by applying Eq.(8).

Typical examples of photographs taken by the schlieren apparatus using the focal filament method are reported in Fig. 5. As explained in Section 3.1, the thin line visible in the ribbed channel identifies the zones of fluid that give rise to a known light ray angular deflection (related to the displacement of the focal filament from its original reference position). In order to detect angular deflections of rays passing in the vicinity of the heated wall, the focal filament has to be moved (as shown in the sequence of pictures displayed in Fig.5) until the corresponding iso-deflection line generated in the image plane intercepts the wall profile at a given point.

Moreover, qualitative information on the thermal field around the heated plate can be inferred from the schlieren image, recorded using the colour filter, shown in Fig. 6; the artificially coloured fluid regions give, at a glance, a visualization of the growing thermal boundary layer. The same figure reports a schlieren colour image obtained for the same experiment, conducted in air under thermal similarity conditions (same Ra_H) in a geometrically similar system (same number of ribs and P/e) [13]. The colour patterns show only minor differences due to the different Pr numbers in the regions

immediately downstream of each rib, where the stagnation zone, inactive from the heat transfer point of view, appears to be wider for the *Pr*=0.7 (air) case.

3.4 Data reduction

The experimentally determined heat transfer results have been recast in terms of dimensionless groups. Local Nusselt number Nu_x and Rayleigh number Ra_x were respectively evaluated from

$$Nu_x = \frac{hx}{k} \tag{9}$$

$$Ra_x = \frac{\beta g x^3 Pr}{\nu^2}\left(T_w - T_f\right) \tag{10}$$

where k, β, ν, and Pr represent the thermal conductivity, coefficient of expansion, kinematic viscosity and Prandtl number of water, respectively, and g is the acceleration of gravity. All the thermophysical properties were evaluated at the film temperature $½(T_w + T_f)$. A single experimental run has been identified by the Rayleigh number Ra_H, based on the channel height H

$$Ra_H = \frac{\beta g H^3 Pr}{\nu^2}\left(T_w - T_f\right) \tag{11}$$

Experiments were conducted for Ra_H in the 1.4×10^7-1.7×10^7 range.

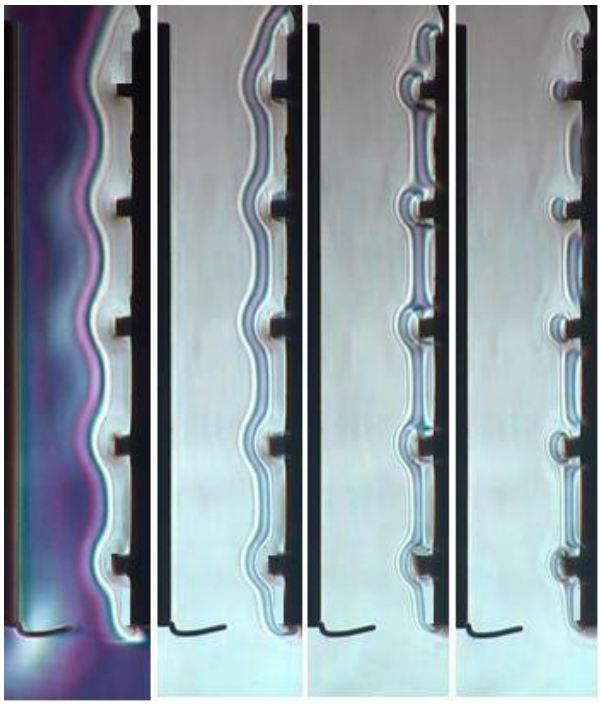

Figure 5 Typical schlieren images recorded with the focal filament progressively moved from its reference position (left-hand image) in order to show the images of points of the optical field deflecting the light by the same known amount (central and right-hand images)

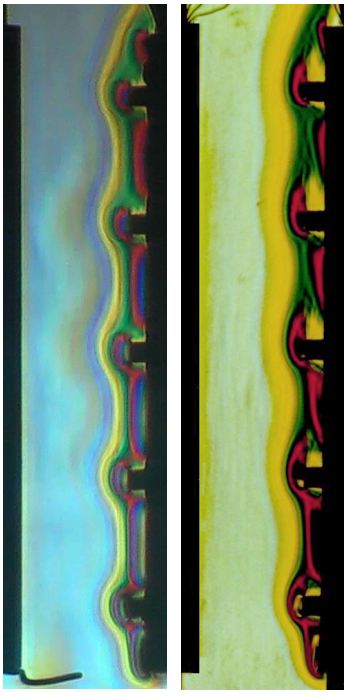

Figure 6 Typical schlieren images recorded with a colour filter. Left-hand: water channel, present work; right-hand: air channel at the same *P/e* and Ra_H values [13]

3.5 Experimental uncertainty

The uncertainty in the results (at the 95% confidence level) was evaluated by using a root-sum-square of the contributions made by the uncertainties in each of the individual measurements, according to the procedures outlined in [16]. The uncertainty in the local heat transfer coefficient h as expressed by Eq.(8) is generally sensitive to the errors associated with the temperature measurements, with the dn/dT relationship assumed for water, and with the schlieren Δ_w readings. As stated by Tanda [12], the accuracy in schlieren Δ_w readings improves with increasing Δ_w, whose value was, for the present experiments, typically between 3 and 6 mm, with associated errors of less than 10%. As errors in the wall-to-fluid temperature difference and dn/dT relationship are accounted for, the uncertainty in h (and Nu_x) values falls into the 15-18% range, while the uncertainty in Ra_x (and Ra_H) is estimated to be 7%.

4. Results and discussion

As mentioned in the Introduction, the aim of the present work was to apply the focal filament schlieren method to measure the local heat transfer coefficient for the buoyancy-induced water flow in an asymmetrically heated, ribbed vertical channel having an aspect ratio S/H equal to 0.2. Heat transfer experiments were performed by keeping the input power, delivered to the heated plate, in the 3 - 4 W range, giving a wall-to-fluid temperature difference of 1.4 to 1.8 K. For values lower than 1.4 K the h-uncertainty related to temperature measurement errors becomes too large; conversely, values higher than 1.8 K give rise to light ray angular deflections too large to be detected by the focal filament (or colour) filter. Depending on the laboratory room temperature, steady-state values of T_w and T_f were in the 19-21°C and 17-20°C ranges, respectively. These experimental conditions were selected in order to achieve the best compromise between schlieren sensitivity and measurement accuracy, and to reproduce, in terms of dimensionless groups, the same conditions considered in a previous experimental investigation conducted using air as convective fluid.

Schlieren images, taken at the steady-state with the colour filter, revealed that the water flow in the channels was always laminar. Under the above mentioned experimental conditions, a large mass of water between the exterior sides of the channels and the tank sides was seemingly featured by no motion; here, the fluid was thermally stratified. Measurements performed by the thermocouple travelling through the fluid showed that the temperature difference between two points, taken in the stagnant fluid and aligned to the inlet and outlet sections of the channels, respectively (i.e. at a vertical distance equal to the channel height H), was typically 0.3-0.4 K, corresponding to about 20-25% of the mean wall-to-fluid temperature difference.

Figure 7 shows a typical distribution of the local heat transfer coefficient h along the heated plate measured for a wall-to-fluid temperature difference of 1.5 K. Different symbols for the inter-rib and the rib (at the center of each vertical side) regions have been adopted. For comparison purposes, the h-distribution obtained in [4] for a smooth vertical channel, by using the same experimental technique, aspect ratio and wall-to-fluid temperature difference, is reported. Inspection of the figure reveals that along the inter-rib regions heat transfer coefficient distribution is characterized by low values close to the ribs, due to the presence of fluid stagnation zones just upstream and downstream of each rib. The space between ribs is sufficient for the main flow to wash the inter-rib surfaces before being deflected by the next rib downstream; this explains the presence of heat transfer coefficient peaks approximately at the midpoint of each inter-rib region. The developing thermal field is responsible for the progressive reduction of h values registered at points separated by an elevation equal to the rib pitch. Relatively high heat transfer coefficients are found on the vertical sides of ribs since they are washed by cool water flow. The heat transfer performance of the ribbed surface is typically lower than that obtained for the smooth surface, with the exception of points located on the ribs close to the channel exit.

Heat transfer coefficient distributions obtained for a larger wall-to-fluid temperature difference (up to 1.8 K) were qualitatively similar in shape, with individual values slightly higher, in line with the typical proportionality between h and $(T_w - T_f)^{0.25}$ occurring in laminar natural convection heat transfer.

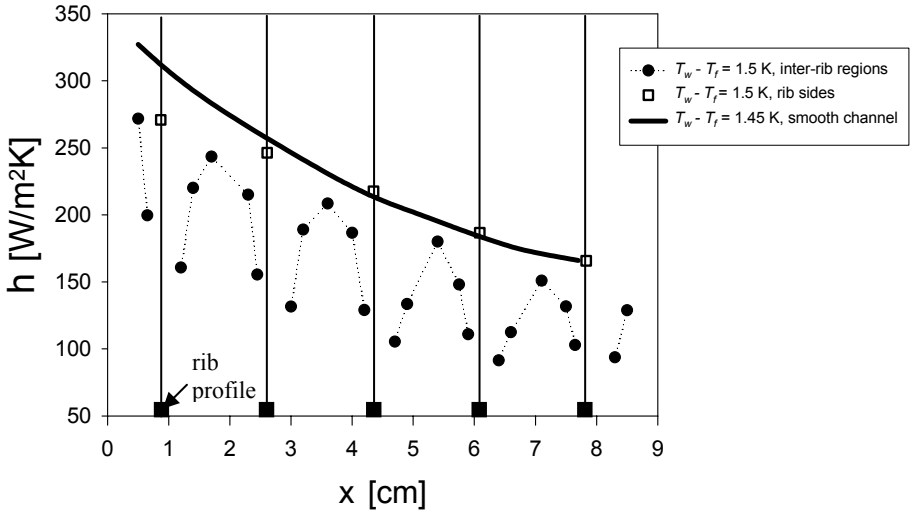

Figure 7 Local heat transfer coefficients along the heated plate with ribs (symbols) and without ribs (continuous line, [4])

Figure 8 reports experimental results presented in the traditional form of local Nusselt number against local Rayleigh number. The same figure displays the experimental results obtained using air (Tanda, [8]) as convective fluid; for the sake of clarity, only the inter-rib regions are considered. The two series of experiments were performed by using the same schlieren technique (focal filament method) and under similarity conditions (almost the same Rayleigh number Ra_H based on the heated plate height H, the same channel aspect ratio S/H, the same number of ribs for each side, the same rib pitch-to-height ratio P/e).

The agreement between dimensionless data recorded for two different Pr-number fluids is excellent and only minor differences are observed. As previously noted in the comment to Fig.6, the highest Pr number fluid (water) produces more effective heat transfer in the recirculation zone downstream of each rib. Moreover, in the case of water, the inter-rib Nu distribution tends to be more uniform and less peaked. This Pr number effect is qualitatively consistent with results obtained in [17] for the forced convection heat transfer in water and air ribbed channels.

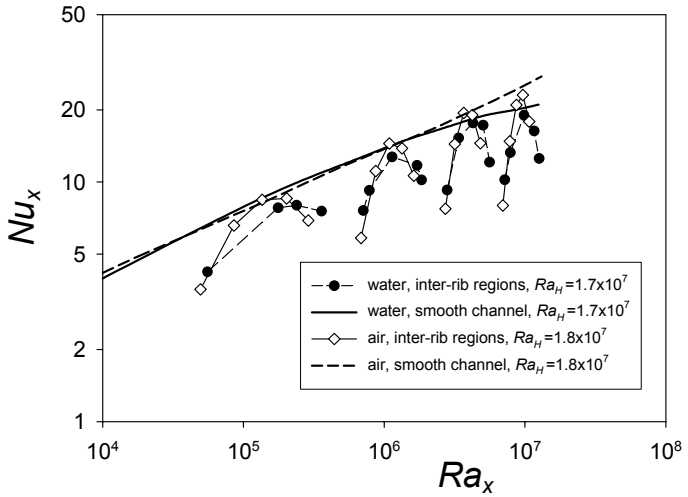

Figure 8 Local Nusselt number versus local Rayleigh number. Full symbols: present experiments for the water ribbed channel, open symbols: experiments for the air ribbed channel (Tanda [8]). Lines: smooth channel experiments for water [4] and air [8]

5. Conclusions

A schlieren technique for the study of convective heat transfer inside vertical channels, with water as working fluid, was presented. This experimental technique, typically employed for quantitative investigations in gases, has been successfully applied here for a liquid.

The investigated channel geometry consisted of an isothermal ribbed heated wall delimited by two, symmetrically arranged, unheated walls. The channel aspect ratio was kept fixed and equal to 0.2.

Local heat transfer coefficients, recorded along the heated side of the ribbed channel, displayed a distribution affected by thermally inactive regions just upstream and downstream of each rib, with heat transfer performance lower than that of the corresponding smooth channel. The same result was obtained using air as working fluid in a previous literature study.

The measurements performed confirm the validity of the schlieren method as quantitative diagnostic tool and encourages its use for the study of thermal fields not only in gases but even in transparent liquid flows.

References

[1] Foucault L 1859 Mémoire sur la construction des télescopes en verre argenté *Annales de l'Observatoire Impérial de Paris* **5** 197-237
[2] Toepler A 1864 *Beobachtungen nach einer neuen optischen Methode – Ein Beitrag zur Experimentalphysik* (M.Cohen & Son)
[3] Settles GS 2001 *Schlieren and Shadowgraph Techniques* (Springer)
[4] Tanda G, Misale M and Fossa M 2014 Heat transfer measurements in water using a schlieren technique *Int. J. Heat Mass Transfer* **71** 451-458
[5] Misale M, Fossa M and Tanda G 2014 Investigation of free convection in a vertical water channel *Exp. Thermal Fluid Science* **59** 252-257
[6] Bhavnani SH and Bergles AE 1990 Effect of surface geometry and orientation on laminar natural convection heat transfer from a vertical flat plate with transverse roughness elements *Int. J. Heat Mass Transfer* **33** 965-981
[7] Aydin M 1997 Dependence of the natural convection over a vertical flat plate in the presence of the ribs *Int. Comm. Heat Mass Transfer* **24** 521-531
[8] Tanda G 1997 Natural convection heat transfer in vertical channels with and without transverse square ribs *Int. J. Heat Mass Transfer* **40** 2173-2185
[9] Onbasioglu SU and Onbasioglu H 2004 On enhancement of heat transfer with ribs *Applied. Thermal Engineering* **24** 43-57
[10] Imbriale M, Panelli M and Cardone G 2012 Heat transfer enhancement of natural convection with ribs *Quantitative Infrared Thermography J.* **9** 55-67
[11] Harvey AH, Gallagher JS and Levelt Sengers JMH 1998 Revised formulation for the refractive index of water and steam as a function of wavelength, temperature and density *J. Physical Chemical Ref. Data* **27** 761-774
[12] Tanda G 1993 Natural convection heat transfer from a staggered vertical plate array *ASME J. Heat Transfer* **115** 938-945
[13] Tanda G 1996 *Application of Optical Methods to the Study of Convective Heat Transfer in Rib-Roughened Channels* Ph.D. Thesis (The City University, London, UK)
[14] Tanda G 2008 Natural convective heat transfer in vertical channels with low-thermal-conductivity ribs *Int. J. Heat Fluid Flow* **29** 1319-1325
[15] Vasil'ev LA 1971 *Schlieren Methods* (Keter Inc)
[16] Moffat RJ 1988 Describing the uncertainties in experimental results *Exp. Thermal Fluid Science* **1** 3-17
[17] Webb BW and Ramadhyani S 1985 Conjugate heat transfer in a channel with staggered ribs *Int. J. Heat Mass Transfer* **28** 1679-1687